Formation and Thermal Stability of Amorphous Phase in Transition Metal-Phosphorus Binary Alloys

Formation and Thermal Stability of Amorphous Phase in Transition Metal-Phosphorus Binary Alloys*

Masaaki Naka**, Akihisa Inoue and Tsuyoshi Masumoto

The Research Institute for Iron, Steel and Other Metals

(Received April 30, 1981)

Synopsis

This paper deals with the amorphous-forming ability of Mn-P, Fe-P, Co-P, Ni-P, Cu-P, Pd-P and Pt-P binary alloys quenched rapidly from the melt and the stability and structural change of the amorphous phases on heating. A melt-quenching technique yields the formation of an amorphous phase only for $Fe_{82.5}P_{17.5}$, $Ni_{81}P_{19}$, $Pd_{81}P_{19}$ and $Pt_{80}P_{20}$ alloys. The critical cooling rate for the formation of an amorphous phase is calculated to be of the order 10^5-10^6 K/s for these amorphous-forming alloys from the transformation theories of crystal nucleation and growth kinetics in the liquid. Therefore, it may be stated that the binary alloys with the critical cooling rates lower than about 10^7 K/s can be melt-quenched to the amorphous state by the centrifugal quenching apparatus used in the present work. Further, it has been demonstrated that the crystallization of these amorphous phases occurs through the two stages of Am. $\longrightarrow$ Am. + Crys-I $\longrightarrow$ Crys-I + Crys-II $\longrightarrow$ Stable Phases near the temperatures of about 620 K for $Fe_{82.5}P_{17.5}$, 600 K for $Ni_{81}P_{19}$, 535 K for $Pd_{81}P_{19}$ and 470 K for $Pt_{80}P_{20}$ alloy.

I. Introduction

Amorphous metallic materials produced by rapid quenching from the liquid have aroused increasing interest owing to its valuable properties in mechanical, physical and chemical fields. These amorphous alloys may be roughly classified into two categories from the alloy composition. One is the early transition metal alloyed with a late transition metal and the other is the alloys consisting of transition metal and metalloid element. Most of amorphous alloys, which have attracted at-

---

* The 1721th report of the Research Institute for Iron, Steel and Other Metals.

** Welding Research Institute, Osaka University, Suita, Osaka 565.

tention as an engineering material, belong to the latter type[1] and they always contain about 15-30 at% metalloid elements (e.g., phosphorus, silicon, carbon and/or boron). Therefore, it is very important to obtain an information on the amorphous-forming ability of the transition metal-based binary alloys containing only one species of these metalloid elements and the stability of their amorphous phases. The first purpose of the present work is to examine the as-quenched structure of transition metal (Mn, Fe, Co, Ni, Cu, Pd or Pt)-based binary alloys containing only phosphorus as metalloid element and to estimate the critical cooling rate for the formation of an amorphous phase. The second is to clarify the stability and structural change of the amorphous phase upon heating.

II. Experimental

Binary alloys of $Mn_{86.9}P_{13.1}$, $Fe_{82.5}P_{17.5}$, $Co_{80.1}P_{19.9}$, $Ni_{81}P_{19}$, $Cu_{83.9}P_{16.1}$, $Pd_{81}P_{19}$ and $Pt_{80}P_{20}$ corresponding to the eutectic composition in each alloy system[2,3] were prepared by melting high purity metallic powder and reagent grade red phosphorus powder. The number of compositions denotes the chemically analyzed compositions in atomic percent. About 100 mg sample of each alloy was melt-quenched using a centrifugal quenching apparatus[4]. Typically, the rotation speed of the drum (10 cm in diameter) was about 5000 rpm and the inner hole diameter of the quartz nozzle was about 0.2 mm. The microstructures of the quenched ribbons were examined by conventional x-ray diffraction and transmission electron microscopy techniques. The thin part of the sample was used without electropolishing for the observation of microstructures by means of an electron microscope. The stability and structural change of an amorphous phase upon heating were examined by a differential thermal analyzer(DTA) at a heating rate of about 5 K/min and an electron microscope with a hot stage. Also, the variation of the electrical resistance during heating was measured by the conventional four-probe technique.

III. Results

1. As-quenched structure

Figure 1 shows the transmission electron micrographs and the selected area diffraction patterns of the melt-quenched alloys. $Mn_{86.9}P_{13.1}$(a), $Co_{80.1}P_{19.9}$(c) and $Cu_{83.9}P_{16.1}$(e) alloys reveal the microcrystalline structures with fine grain sizes of about 100 nm. The diffraction patterns indicate the existence of the mixed structures con-

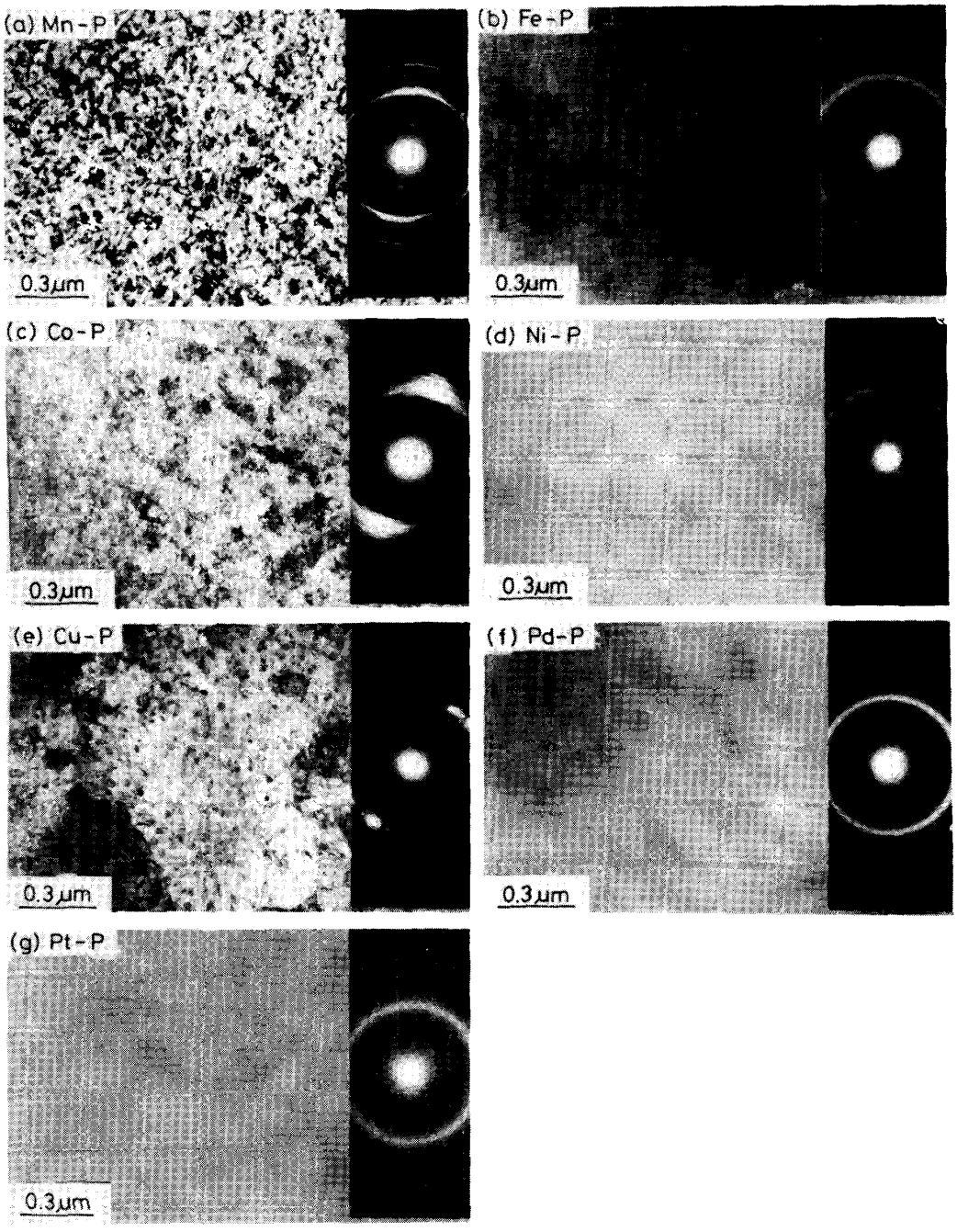

Fig. 1 Transmission electron micrographs and selected area diffraction patterns showing the as-quenched structure of transition metal-phosphorus alloys. (a) $Mn_{86.9}P_{13.1}$, (b) $Fe_{82.5}P_{17.5}$, (c) $Co_{80.1}P_{19.9}$, (d) $Ni_{81}P_{19}$, (e) $Cu_{83.9}P_{16.1}$, (f) $Pd_{81}P_{19}$ and (g) $Pt_{80}P_{20}$.

sisting of each mother metal and phosphide. On the other hand, $Fe_{82.5}P_{17.5}$(b), $Ni_{81}P_{19}$(d), $Pd_{81}P_{19}$(f) and $Pt_{80}P_{20}$(g) alloys indicate the results on the formation of an amorphous phase; namely, the bright field images give the featureless contrast and the corresponding diffraction patterns show only a few diffused haloes. The positions of the first and second peaks on the diffraction pattern represented by $\sin\theta/\lambda$ were 0.239 and 0.414 A^{-1} for $Fe_{82.5}P_{17.5}$, 0.247 and 0.434 A^{-1} for $Ni_{81}P_{19}$, 0.244 and 0.382 A^{-1} for $Pd_{81}P_{19}$ and 0.209 and 0.546 A^{-1} for $Pt_{80}P_{20}$, respectively.

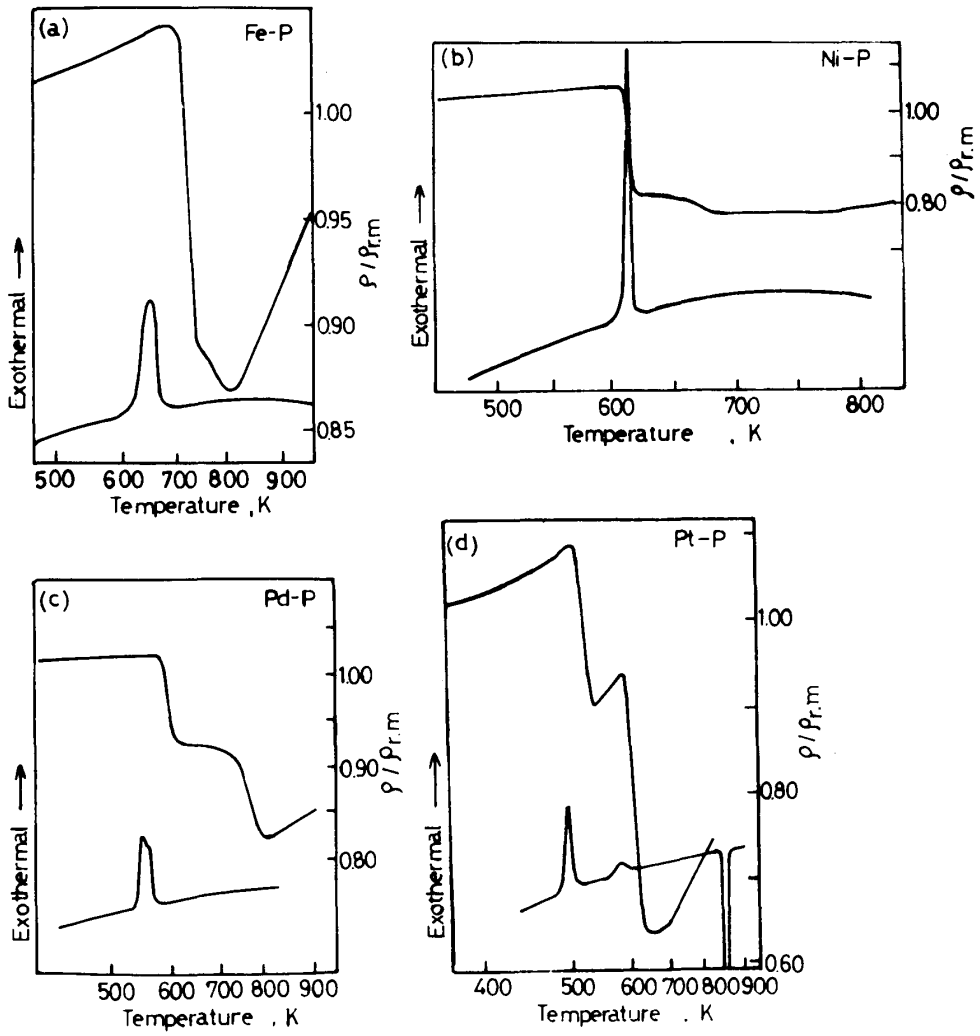

Fig. 2 Differential thermal analysis curves and relative electrical resistance ($\rho/\rho_{r.m}$) curves during heating, where $\rho_{r.m}$ is the electrical resistivity at room temperature. (a) $Fe_{82.5}P_{17.5}$, (b) $Ni_{81}P_{19}$, (c) $Pd_{81}P_{19}$ and (d) $Pt_{80}P_{20}$ amorphous alloys.

2. Thermal stability and crystallization behavior

Figure 2 shows the DTA curves and the relative electrical resistance curves during heating. The crystallization starts at the temperature where a sharp exothermic peak on the DTA curve and a sharp drop on the electrical resistance curve occur. The crystallization temperatures defined as the beginning point of the first exothermic peak on DTA curves were determined to be 621 K for $Fe_{82.5}P_{17.5}$, 601 K for $Ni_{81}P_{19}$, 533 K for $Pd_{81}P_{19}$ and 471 K for $Pt_{80}P_{20}$ alloy, respectively.

The crystallization behaviors during heating for these four amorphous alloys were examined mainly by transmission electron microscopy. In all the alloys except $Pd_{81}P_{19}$ alloy it has been found that the crystallization proceeds with the sequence of Am. $\rightarrow$ Am. + Crys-I $\rightarrow$ Crys-I + Crys-II $\rightarrow$ Stable Phases. As examples, the electron micrographs of $Fe_{82.5}P_{17.5}$, $Ni_{81}P_{19}$ and $Pt_{80}P_{20}$ alloys heated on the hot stage of an electron microscope are shown in Figs. 3 to 5, respectively. The featureless contrast of amorphous structures shown in the photographs (a) remains unchanged up to about 600 K for the Fe-P alloy, 580 K for the Ni-P alloy and 440 K for the Pt-P alloy. With further heating up to temperatures near the crystallization temperature, a globular or elliptic microcrystal precipitates numerically over the entire area of amorphous phase, as seen in the photographs (b). The growth rate of this crystal is relatively slow and the average sizes in diameter are less than about 15 nm for all the alloys. The corresponding diffraction pattern indicates that this crystalline phase named as Crys-I is a b.c.c. structure for $Fe_{82.5}P_{17.5}$ and a f.c.c. structure for $Ni_{81}P_{19}$ and $Pt_{80}P_{20}$ alloy. With further heating up to the temperatures slightly higher than the crystallization temperatures, an oval-shaped crystal named as Crys-II appears and grows rapidly in the remaining amorphous phase (the photographs c) and then complete transformation occurs as shown in the photographs (d) to (f). The Crys-II phase was identified to be a M_3P type compound with a b.c. tetragonal structure[5], e.g., Fe_3P for the Fe-P alloy, Ni_3P for the Ni-P alloy and Pt_3P for the Pt-P alloy. On the other hand, the $Pd_{81}P_{19}$ amorphous alloy transformed directly to Pd_3P compound with a b.c. tetragonal structure (Crys-II) without the appearance of the Crys-I phase, as shown in Fig. 6. The above-described crystallization behaviors are almost the same as those of amorphous (Fe, Co, Ni)-Si-B ternary and quaternary alloys[6,7].

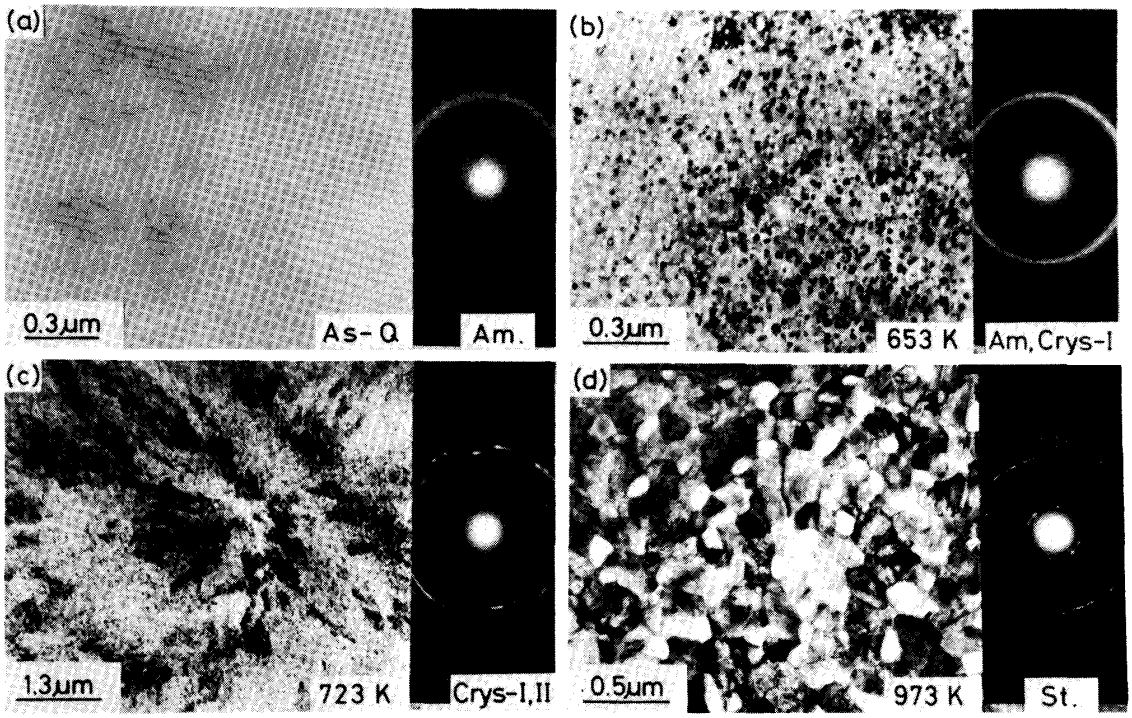

Fig. 3 Transmission electron micrographs and selected area diffraction patterns showing the crystallization of amorphous $Fe_{82.5}P_{17.5}$ alloy heated on the hot stage of an electron microscope.

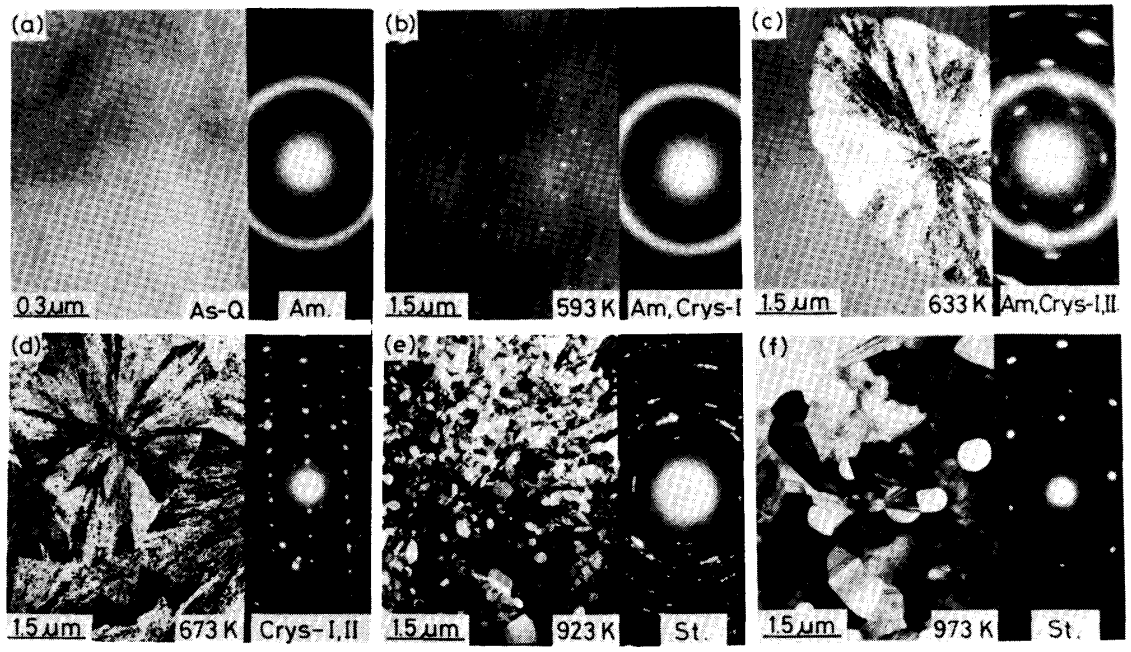

Fig. 4 Transmission electron micrographs and selected area diffraction patterns showing the crystallization of amorphous $Ni_{81}P_{19}$ alloy heated on the hot stage of an electron microscope.

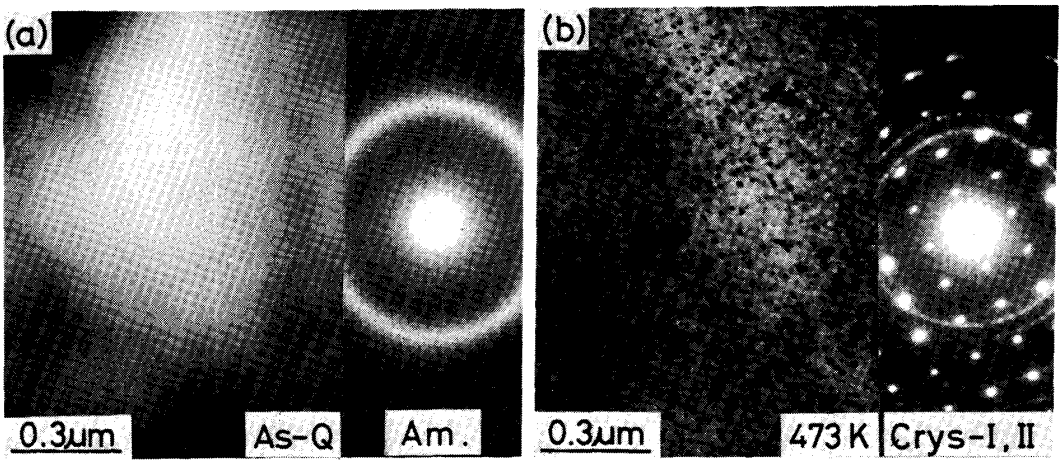

Fig. 5 Transmission electron micrographs and selected area diffraction patterns showing the crystallization of amorphous $Pt_{80}P_{20}$ alloy heated on the hot stage of an electron microscope.

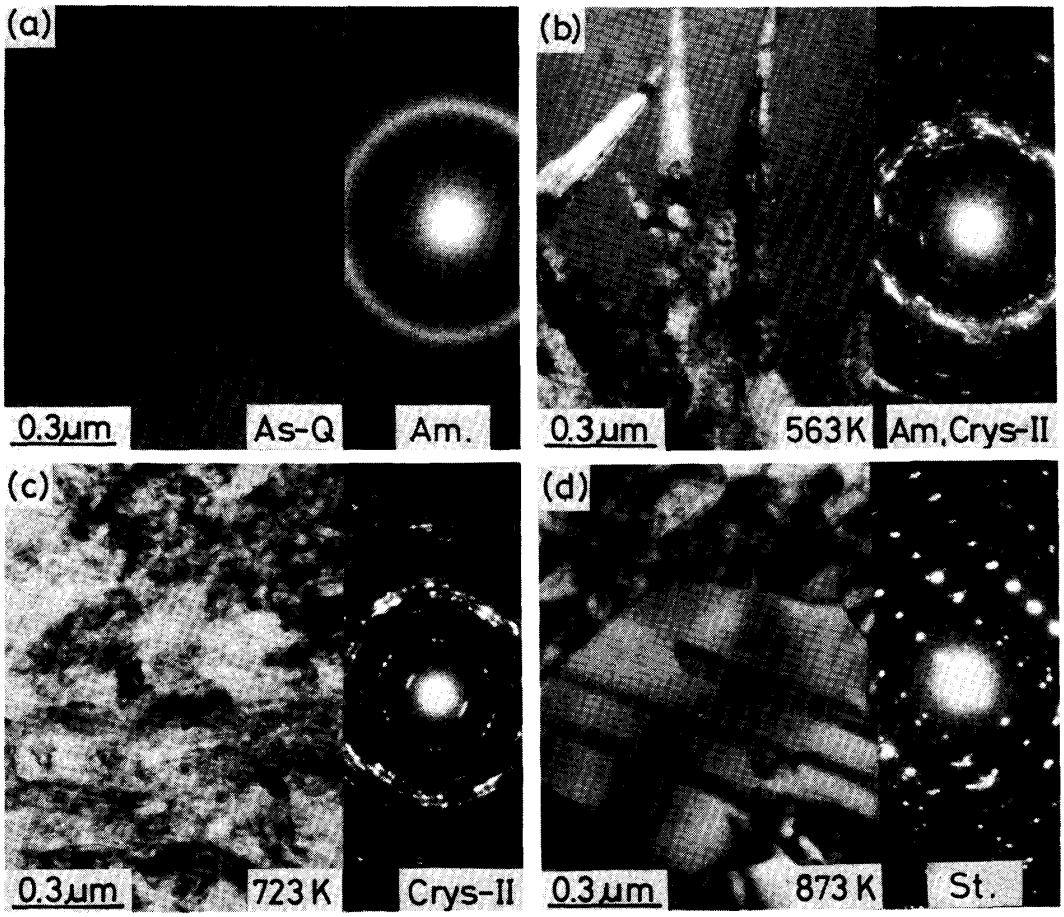

Fig. 6 Transmission electron micrographs and selected area diffraction patterns showing the crystallization of amorphous $Pd_{81}P_{19}$ alloy heated on the hot stage of an electron microscope.

IV. Discussion

The present results demonstrate that the application of melt-quenching to (Mn, Fe, Co, Ni, Cu, Pd or Pt)-P binary alloys yields the formation of the amorphous phase for $Fe_{82.5}P_{17.5}$, $Ni_{81}P_{19}$, $Pd_{81}P_{19}$ and $Pt_{80}P_{20}$ alloys and of the crystalline phases for $Mn_{86.9}P_{13.1}$, $Co_{80.1}P_{19.9}$ and $Cu_{83.9}P_{16.1}$ alloys.

Davies et al.[8] have calculated the critical cooling rate for the formation of an amorphous single phase, based on the assumption that any metallic liquid firms an amorphous phase if it is supercooled rapidly below a glass transition temperature without the crystallization. According to the transformation theories of crystal nucleation and grwoth in the liquid, the time t for the crystallization of a small volume fraction x in a congruently melting system at a temperature T is given by the following equation:

$$t = \frac{9.32\eta}{kT} \left\{ \frac{a^9 \; x \; \exp(1.024/T_r{}^3 \Delta T_r{}^2)}{f^3 \; N_V \; [1-\exp(-\Delta H_f^m \; T_r/RT)]^3} \right\}^{1/4} \qquad (1)$$

where a is the average atomic diameter, N_V the number of atoms per unit volume, $T_r = T/T_m$, $\Delta T_r = (T_m - T)/T_m$, T_m the melting temperature, ΔH_f^m the heat of fusion per mole, η the viscosity at temperature T and f the fraction of sites where atoms may be preferentially added or removed. For the alloys with small entropies of fusion (<2R) such as $Fe_{82.5}P_{17.5}$, $Ni_{81}P_{19}$ and $Pt_{80}P_{20}$, the interface is expected to be close and hence it was assumed that f = 1. On the other hand, $Pd_{81}P_{19}$ alloy is inferred to solidify to two intermetallic compounds Pd_5P and Pd_3P[9], it was assumed that $f = 0.2 \; \Delta T_r$[8]. Further, x is taken to be 10^{-6}.

The critical cooling rate for amorphous phase formation, R_c, is approximated by the linear cooling rate required to avoid the nose of the time-temperature-transformation (T-T-T) curves constructed by using Eq.(1) and is given by

$$R_c = \frac{T_m - T_n}{t_n} \qquad (2)$$

where T_n and t_n are the temperature and time, respectively, corresponding to the nose of T-T-T curve. There is little information on the experimental data of viscosities for molten amorphous-forming alloys and hence the liquid viscosities at high temperatures for $Fe_{82.5}P_{17.5}$, $Co_{80.1}P_{19.9}$, $Ni_{81}P_{19}$ and $Cu_{83.9}P_{16.1}$ alloys were estimated from the extrapolated value by Arrhenius-plotting the viscosities for the pure liquid of iron, cobalt, nickel or copper[10]. Using the viscosity data at high temperatures, smooth interpolations are achieved between melting temperature T_m and glass transition temperature T_g as shown in Fig. 7. The glass transition temperatures of the binary amorphous alloys were

assumed to be equal to the observed crystallization temperatures. Additionally, the glass transition temperatures of $Mn_{86.9}P_{13.1}$, $Co_{80.1}P_{19.9}$ and $Cu_{83.9}P_{16.1}$ alloys were estimated from the empirical relation $T_x/T_m \simeq T_g/T_m = 0.51$ derived for $Fe_{82.5}P_{17.5}$, $Ni_{81}P_{19}$, $Pd_{81}P_{19}$ and $Pt_{80}P_{20}$ alloys. Further, the ΔH_f^m values of the alloys were estimated from the relation $\Delta H_f^m = 2.3\ T_m$[11].

Figure 8 shows the T-T-T curves constructed based on the above approximations. Table I lists the critical cooling rates, R_c, for the amorphous phase formation of the binary transition metal-phosphorus alloys. The R_c values of Fe-P, Ni-P, Pd-P and Pt-P alloys calculated by Davies et al.[8] are also represented for comparison. Table I demonstrates that these binary alloys possess individually different critical cooling rates for the amorphous phase formation and the alloys exhibiting the critical cooling rates less than about 5×10^6 K/s can form the amorphous phase. Also, this result suggests that the cooling rate of the order 10^6 - 10^7 K/s is the maximum cooling rate of the sample achieved by the present apparatus[12]. That is, the alloys do not exhibit the amorphous phase when the critical cooling rate for the amorphous phase formation of alloys are higher than about 10^7 K/s. Further, the calculated R_c values suggest that the amorphous-forming ability is the largest for $Pt_{80}P_{20}$ followed by $Pd_{81}P_{19}$, $Ni_{81}P_{19}$ and then $Fe_{82.5}P_{17.5}$

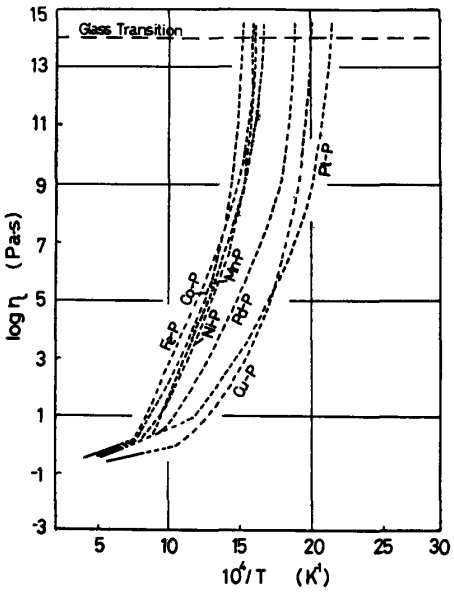

Fig. 7 Hypothetical viscosity-temperature relations for liquid $Mn_{86.9}P_{13.1}$, $Fe_{82.5}P_{17.5}$, $Co_{80.1}P_{19.9}$, $Ni_{81}P_{19}$, $Cu_{83.9}P_{16.1}$, $Pd_{81}P_{19}$ and $Pt_{80}P_{20}$ alloys, in the temperature ranges between the respective melting temperatures and glass transition temperatures.

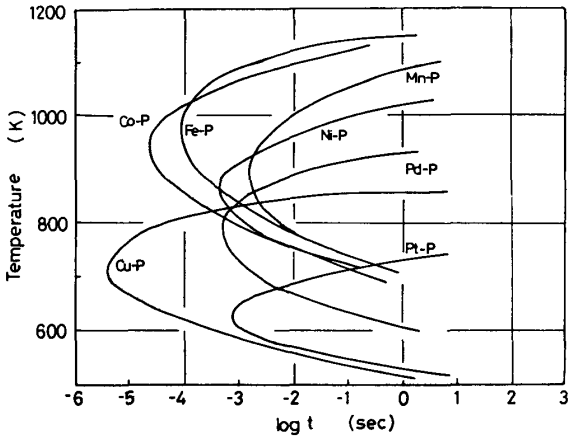

Fig. 8 Time-Temperature-Transformation curves for $Mn_{86.9}P_{13.1}$, $Fe_{82.5}P_{17.5}$, $Co_{80.1}P_{19.9}$, $Ni_{81}P_{19}$, $Cu_{83.9}P_{16.1}$, $Pd_{81}P_{19}$ and $Pt_{80}P_{20}$ alloys corresponding to a volume fraction crystallized to 10^{-6}.

Table I Critical cooling rates for the formation of the amorphous phase of transition metal-phosphorus binary alloys.

Alloy composition	R_c(K/s)	R_c*(K/s)
$Mn_{86.9}P_{13.1}$	2.0×10^5	
$Fe_{82.5}P_{17.5}$	4.6×10^6	3.2×10^6
$Co_{80.1}P_{19.9}$	1.4×10^7	
$Ni_{81}P_{19}$	6.3×10^5	7.9×10^5
$Cu_{83.9}P_{16.1}$	7.4×10^7	
$Pd_{81}P_{19}$	5.4×10^5	2.0×10^5
$Pt_{80}P_{20}$	3.3×10^5	6.3×10^5

* Calculated by Davies et al.[13)]

alloys. Although the $Pt_{80}P_{20}$ alloy possesses the highest amorphous-forming ability, the melt-quenched sample often showed a slight existence of crystallites precipitated from the amorphous phase during cooling after the formation of amorphous single phase, owing to the low crystallization temperature of $Pt_{80}P_{20}$. The discrepancy between the calculated R_c value and the actual amorphous-forming ability for $Mn_{86.9}P_{13.1}$ alloy may be due to the ease of oxidation of the Mn-rich alloy because the melt quenching was made in air. Hence, the $Mn_{86.9}P_{13.1}$ alloy could be quenched to the amorphous state if the oxidation of sample during cooling was prevented. The quenched $Co_{80.1}P_{19.9}$ alloy does not exhibit any trace of amorphous phase even though the alloy possesses almost the same melting temperature as that of $Fe_{82.5}P_{17.5}$ alloy. Such a difference of amorphous-forming ability may be attributed to lower viscosities in the supercooled liquid of $Co_{80.1}P_{19.9}$ alloy. Similarly, $Cu_{83.9}P_{16.1}$ alloy cannot be quenched to the amorphous state because of its high critical cooling rate due to extremely low viscosities of the supercooled liquid.

V. Summary

The microstructures of melt-quenched binary alloys, $Mn_{86.9}P_{13.1}$, $Fe_{82.5}P_{17.5}$, $Co_{80.1}P_{19.9}$, $Ni_{81}P_{19}$, $Cu_{83.9}P_{16.1}$, $Pd_{81}P_{19}$ and $Pt_{80}P_{20}$, were investigated by x-ray diffraction method and electron microscopy. The crystallization behaviors of the alloys, which showed amorphous structure, were also examined with differential thermal analysis and electrical resistance measurements. The results obtained are summarized

as follows:

(1) The amorphous phase was obtained for $Fe_{82.5}P_{17.5}$, $Ni_{81}P_{19}$, $Pd_{81}P_{19}$ and $Pt_{80}P_{20}$ alloys, while $Mn_{86.9}P_{13.1}$, $Co_{80.1}P_{19.9}$ and $Cu_{83.9}P_{16.1}$ alloys consisted of two crystalline phases. The crystallization of the amorphous phase occurred through the two stages, e.g., Am. $\longrightarrow$ Am. + Crys-I $\longrightarrow$ Crys-I + Crys-II $\longrightarrow$ Stable Phases, near the temperatures of 620 K for the Fe-P alloy, 600 K for the Ni-P alloy, 535 K for the Pd-P alloy and 470 K for the Pt-P alloy.

(2) The critical cooling rate for the formation of an amorphous phase was calculated using the transformation theories of crystal nucleation and grwoth kinetics in the liquid. The critical cooling rate was the highest (4.6×10^6 K/s) for $Fe_{82.5}P_{17.5}$ followed by 6.3×10^5 K/s for $Ni_{81}P_{19}$, 5.4×10^5 K/s for $Pd_{81}P_{19}$ and then 3.3×10^5 K/s for $Pt_{80}P_{20}$ alloy. Therefore, it is concluded that the binary alloys with the critical cooling rates lower than about 10^7 K/s can be melt-quenched to the amorphous state.

References

(1) For example, F.E. Luborsky and L.A. Johnson, J. de Phys., Colloque -8, 41 (1980), 820.

(2) Metals Handbook, 8th ed., Metallography, Structures and Phase Diagrams, ASM, Metals Park, Ohio, 1973.

(3) C.J. Smithells, Metals Reference Book, 5th ed., Butterworths, London, (1976).

(4) R. Pond and R. Maddin, Trans. Met. Soc. AIME, 245 (1969), 2475.

(5) W.B. Pearson, Handbook of Lattice Spacings and Structures of Metals and Alloys, Pergamon Press, Oxford, (1958).

(6) T. Masumoto, A. Inoue and H.M. Kimura, J. Japan Inst. Metals, 41 (1977), 730.

(7) A. Inoue, T. Masumoto, M. Kikuchi and T. Minemura, J. Japan Inst. Metals, 42 (1978), 294; Sci. Rep. RITU, A27 (1979), 127.

(8) H.A. Davies, J. Aucote and J.B. Hull, Scripta Met., 8 (1974), 1179.

(9) M. Hansen, Constitution of Binary Alloys, McGraw-Hill, New York, (1958), p. 1084.

(10) S.W. Strauss, Nucl. Sci. Eng., 12 (1962), 436.

(11) Data Book of Metals, Japan Inst. Metals ed., Maruzen, Tokyo, (1974), p. 11.

(12) P. Predecki, A.W. Mullendore and N.J. Grant, Trans. Met. Soc. AIME, 233 (1965), 1581.

(13) H.A. Davies and B.G. Lewis, Scripta Met., 9 (1975), 1107.